From Model Compounds to Extended π-Conjugated Systems: Synthesis and Properties of Dithieno[3,2-*b*:2′,3′-*d*]phospholes

Thomas Baumgartner,*[a] Werner Bergmans,[a] Tamás Kárpáti,[b] Toni Neumann,[a] Martin Nieger,[c] and László Nyulászi*[b]

Abstract: To explore their suitability for applications in molecular optoelectronics and as sensory materials, novel dithieno[3,2-*b*:2′,3′-*d*]phospholes have been synthesized and their reactivity and properties investigated. An efficient two-step synthesis allowed for a modular assembly of differently functionalized compounds. The dithieno[3,2-*b*:2′,3′-*d*]phosphole system exhibits extraordinary optoelectronic properties with respect to wavelength, intensity, and tunability. Owing to the nucleophilic nature of the central phosphorus atom, its significant electronic influence on the conjugated π system can be altered selectively by chemically facile modifications such as oxidation or complexation with Lewis acids or transition metals. All the dithienophosphole species presented show very strong blue photoluminescence with excellent quantum yield efficiencies supporting their potential utility as blue-light emitting components in organic light emitting diodes (OLEDs). Furthermore, depending on the electronic nature of the phosphorus center, the materials exhibit distinctive optoelectronic properties suggesting that the dithieno[3,2-*b*:2′,3′-*d*]phosphole system may be useful as sensory material. Theoretical calculations, including time-dependent DFT methods, revealed the excellent predictability of the structures and optoelectronic properties of the functionalized dithienophospholes allowing the design of future dithieno[3,2-*b*:2′,3′-*d*]phosphole-based materials to be "stream-lined". By using tin-functionalized dithienophosphole monomers, a strategy, which involves Stille coupling, towards extended π-conjugated materials with significantly redshifted optoelectronic properties is also presented.

Keywords: density functional calculations · luminescence · molecular electronics · optical properties · phosphorus heterocycles

Introduction

The incorporation of phosphorus centers into oligomeric or macromolecular materials is currently receiving increasing amounts of interest.[1] The versatile reactivity and electronic nature of phosphorus offers interesting opportunities for the development of new materials with novel properties. Phosphole-containing systems are of particular interest in molecular electronics as materials that possess the structurally related pyrrole and thiophene moieties are already well-established in this field.[2] The corresponding phosphole-containing materials have great potential for applications in electronic devices such as photovoltaic cells, organic or polymer light-emitting diodes (OLEDs or PLEDs), polymeric sensors, and organic thin-film transistors (OTFTs).[3] Recently, Réau and co-workers, who incorporated the phosphole moiety into extended thiophene-containing π-conjugated systems (**P1**), demonstrated the advantageous electronic features of these phosphorus-containing systems which allow selective fine-tuning of the electronic structure of the mate-

[a] Dr. T. Baumgartner, W. Bergmans, T. Neumann
Institute of Inorganic Chemistry, RWTH-Aachen University
Landoltweg 1, 52074 Aachen (Germany)
Fax: (+49) 241-809-2644
E-mail: thomas.baumgartner@ac.rwth-aachen.de

[b] Dr. T. Kárpáti, Prof. L. Nyulászi
Department of Inorganic Chemistry
Technical University of Budapest
1521 Budapest Gellért tér 4 (Hungary)
Fax: (+36) 1463-3462
E-mail: nyulaszi@mail.bme.hu

[c] Dr. M. Nieger
Institut für Anorganische Chemie, Universität Bonn
Gerhard-Domagk-Strasse 1, 53121 Bonn (Germany)

Supporting information for this article is available on the WWW under http://www.chemeurj.org/ or from the author. It contains tables of relevant bond lengths for **10b**, **11**, and **13** determined by single-crystal X-ray structure studies, selected bond lengths and Bird indices for the investigated species (**S2b**, **T1**–**T4**) calculated at the B3LYP/6-31G* level of theory and TD-DFT-calculated optical spectroscopy data.

 DOI: 10.1002/chem.200500152

rials.[1f,4] Owing to the pyramidal nature of the tricoordinate phosphorus center, an efficient interaction of its lone-pair orbital with the conjugated π system is inhibited resulting in only a small amount of lone-pair delocalization. A weak interaction can, however, be observed between the π* LUMO and the exocyclic σ^*_{PC} orbital. Therefore, the lone pair at the phosphorus atom functions as a kind of dopant in the π system rather than being an integral part of the aromatic system. Conveniently, the electronic structure of the π-conjugated system can be efficiently controlled by simple chemical modifications, such as the oxidation or complexation of the phosphorus center.[1f,4] Although these intriguing features, in addition to theoretical calculations,[5] strongly support the advantages of the incorporation of phosphole moieties into extended oligomeric or macromolecular systems, only a few examples of phosphole-containing systems have been reported to date: The first oligomeric phosphole-containing materials **P2** and **P3** were reported by Mathey and co-workers in the early 1990s,[6] whereas the first example of a macromolecular phosphole system **P4** was only reported in 1997 by Mao and Tilley.[7a] Recently, Réau and co-workers accessed the bithiophene-bridged phosphole polymer **P5a** by electropolymerization[1f] and Chujo and co-workers reported the phenylene(ethynylene)-linked material **P5b**.[7b]

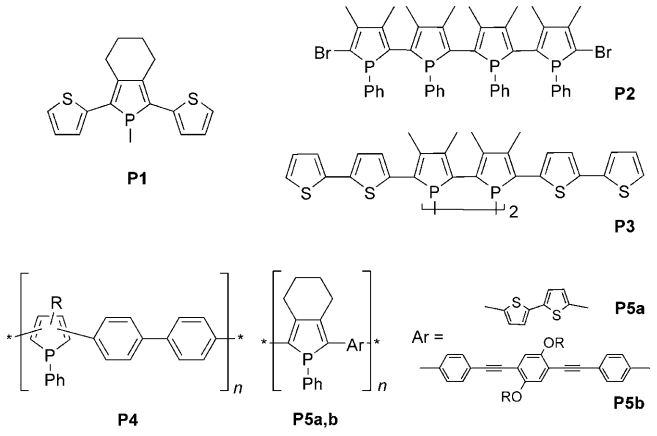

As already indicated, careful consideration of the HOMO–LUMO gap, which strongly influences the optical and electronic properties of materials, is essential for their utility in molecular electronics.[8] In this context, Ohshita and co-workers have shown, for example, that the incorporation of a silicon bridge into a bithienyl moiety reduces the HOMO–LUMO gap of the material (**S1**) significantly owing to the formation of an extended planar π-conjugated system. This feature could allow the material to be used as a hole-transport material in electroluminescent (EL) devices.[9] However, the number of different dithieno systems is very limited and the only known examples include boron (**S2a**, E = BR),[10] carbon (**S2b**, E = CR_2),[11] nitrogen (**S2c**, E = NR),[12] silicon (**S1**),[13] and sulfur (**S2d–f**, E = $S(=O)_{0,1,2}$)[14] as bridging elements. The use of phosphorus has only been reported in compound **P6**,[15] whereas σ^3,λ^3-phosphorus-based systems (**P7**), on the other hand, had been completely unknown until recently.

As part of our research into the development of processible, electronically active, macromolecular inorganic materials we focused our attention on the novel dithieno[3,2-

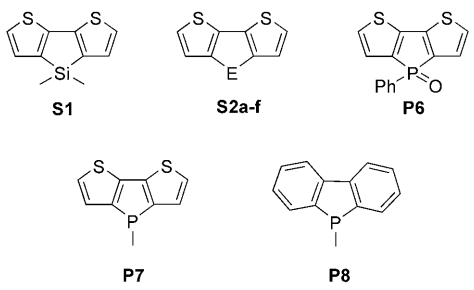

b:2′,3′-*d*]phosphole moiety **P7**.[16] In this system, the molecular framework of the bithienyl moiety is rigidified by a phosphorus bridge to give a new anellated ring system. This system should possess a smaller HOMO–LUMO gap than any of its component rings, as has been observed for related sulfur-bridged thiophene materials.[17] Furthermore, the HOMO–LUMO gap is reduced by the interaction of the π* LUMO with the σ^*_{PC} orbital and the presence of the phosphorus atom allows selective tuning of the electronic properties of the material by its functionalization. Like almost no other element, trivalent phosphorus is particularly suited for the bridging position in the dithieno system owing to its nucleophilic nature. Its ability to react with oxidizing agents, its Lewis basicity, which allows reactions with Lewis acids, in addition to its potential for coordination to transition metals allows the electronic properties of the dithienophosphole materials to be modified by a unique variety of synthetically facile methods. Note that in this context the incorporation of a phosphole unit into a benzo-anellated ring system has been found to further reduce the lone-pair delocalization[18] largely because the benzene subunits tend to retain their aromatic character. Therefore, (di)benzophospholes (**P8**), or dithienophospholes (**P7**) for that matter, cannot be considered classic phospholes; they represent an independent class of compound.[19]

Recently we reported that the novel dithieno[3,2-*b*:2′,3′-*d*]phosphole species **1** (**a**: R = Ph; **b**: R = 4-*t*BuPh) and the corresponding polymeric materials **2** (**a**: E = lone pair; **b**: E = O; TBDMS = *tert*-butyldimethylsilyl) possessed very advantageous properties with respect to wavelength, intensity, tunability, as well as optical and thermal stability.[16a] The dithieno[3,2-*b*:2′,3′-*d*]phosphole moiety is a very efficient emitter of blue light suggesting potential applications in optoelectronic devices such as PLEDs or polymeric sensory materials.

In this paper we report in detail on the synthesis and optoelectronic properties of the dithieno[3,2-*b*:2′,3′-*d*]phosphole system including theoretical calculations. We will discuss the possibilities of tuning the electronic structure of the

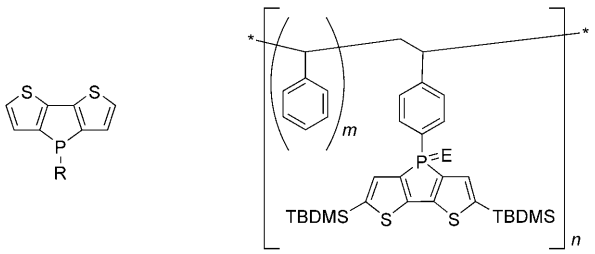

1a,b 2a,b

system by various chemical modifications and thus probe the potential of the dithienophosphole system for use as sensory materials. Furthermore, a route to extended π-conjugated systems containing the dithieno[3,2-*b*:2′,3′-*d*]phosphole moiety is discussed as well.

Results and Discussion

Synthesis and characterization of dithieno[3,2-*b*:2′,3′-*d*]phospholes: By taking into account the properties of the systems described by Ohshita[9,13] and Réau[1f,4] and their coworkers it seemed necessary for us to incorporate an electron acceptor into the dithienophosphole system in order to further optimize the HOMO–LUMO separation. We decided to use silyl groups since they can be easily introduced and exhibit suitable acceptor properties through negative hyperconjugation.[20]

By applying synthetic variations of the strategy by Ohshita et al. for the synthesis of dithienosiloles[9a] to our system, we were able to access novel dithieno[3,2-*b*:2′,3′-*d*]phospholes with the desired silyl functionality. Starting from 3,3′,5,5′-tetrabromobithiophene **3**, the silyl groups were introduced by reaction with *n*-butyllithium followed by the addition of the corresponding chlorosilanes (Me_3SiCl, $tBuMe_2SiCl$) at −78 °C in THF to afford the silyl-functionalized bithiophenes **4**[9a] and **5** in almost quantitative yields (Scheme 1). Subsequent lithiation of **4** and **5** with two equivalents of *n*-butyllithium followed by the addition of $RPCl_2$ (R = Ph, 4-*t*BuPh, *t*Bu) in the presence of *N*,*N*,*N*′,*N*′-tetramethyl-1,2-ethanediamine (TMEDA) cleanly afforded the dithieno[3,2-*b*:2′,3′-*d*]phospholes **6–9** as off-white waxy solids in good yields after filtration through neutral alumina. All four compounds exhibit ^{31}P NMR chemical shifts (**6**: $\delta = -25.0$ ppm; **7**: $\delta = 0.3$ ppm; **8**: $\delta = -27.4$ ppm; **9**: $\delta = -28.2$ ppm) that are significantly shifted upfield relative to those of the phospholes reported by Réau et al. ($\delta^{31}P = 11$–45 ppm),[1f] but in the same range as the non-silyl-functionalized dithienophospholes **1a** and **1b** (cf. **1a**: $\delta^{31}P = -21.5$ ppm; **1b**: $\delta = -22.5$ ppm)[16a] indicating that these silyldithienophospholes are related to dibenzophosphole (cf. $\delta^{31}P = -12.8$ ppm for **P8**; R = Ph)[21] rather than to classic phospholes. The slight upfield shift of the ^{31}P NMR resonances of the aryl-substituted, silyl-functionalized systems relative to their nonfunctionalized congeners supports the further extended π-conjugated system induced by the electron-accepting silicon centers in **6–9**. The ^{1}H and ^{13}C NMR data for **6–9** show the same trends as those observed for the related dithieno systems[9,12] and for the previously reported dithienophospholes.[16]

Derivatization of the dithieno[3,2-*b*:2′,3′-*d*]phosphole system: As mentioned earlier, the unique ability of phosphorus to react with oxidizing agents, its Lewis basicity, which allows reactions with Lewis acids, in addition to its potential for coordination to transition metals, enables a broad range of synthetically facile chemical modifications to be made to tune the electronic properties of the dithienophosphole materials. Note that exploitation of the nucleophilicity of the σ^3,λ^3-phosphorus atom gives rise to a significant increase in the acceptor properties of this center.

Reaction of **6** with oxidizing agents such as H_2O_2 or sulfur in THF at room temperature resulted in the clean formation of the phosphole oxide **10a** and the phosphole sulfide **11**, respectively (Scheme 2). The ^{31}P NMR spectrum of the oxidized species **10a** exhibits a signal at $\delta = 17.2$ ppm, which, as expected for a phosphane oxide, is at a low field relative to that of **6**. However, the value of the chemical shift for **10a** is still upfield-shifted relative to related bis(thienyl)phosphole oxide systems ($\delta^{31}P \approx 45$ ppm),[1f,4] supporting the high degree of π conjugation in the dithieno subunits in **10a**. The same is true for the sulfurized species **11** which has a ^{31}P NMR resonance at $\delta = 23.6$ ppm (cf. $\delta^{31}P \approx 53$ ppm for bis-

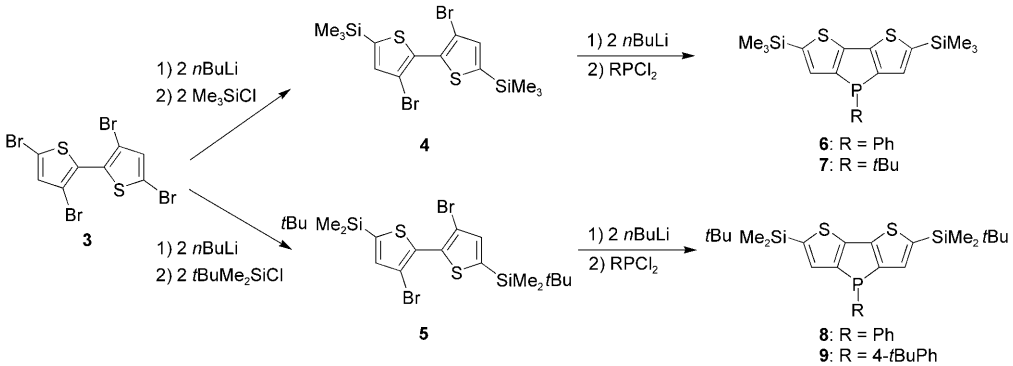

Scheme 1. Synthesis of dithieno[3,2-*b*:2′,3′-*d*]phospholes **6–9**.

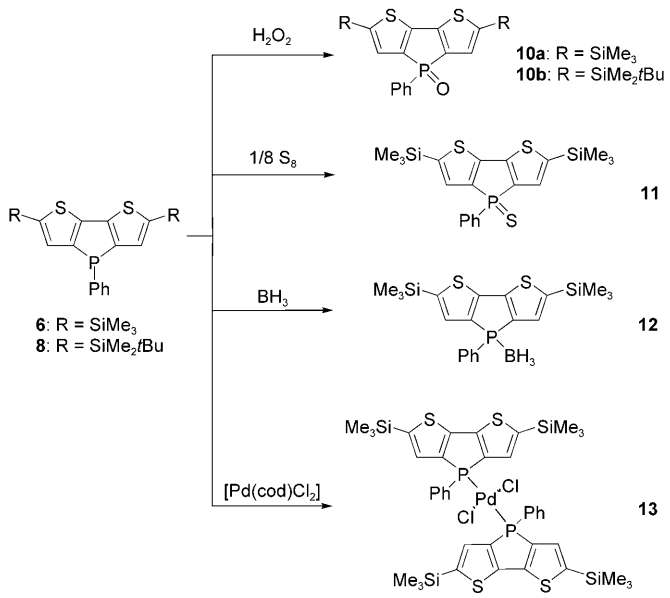

Scheme 2. Functionalization of dithieno[3,2-*b*:2′,3′-*d*]phospholes **6** and **8**.

(thienyl)phosphole sulfides[1f,4]). The ^{1}H and ^{13}C NMR data show the same trend and correlate with the data observed for non-silyl-functionalized dithienophospholes.[16]

We were able to obtain single crystals suitable for X-ray crystal structure studies of **10b**[22] and **11** from concentrated solutions of them in pentane and hexane, respectively, at room temperature. The structural data for both compounds show two independent molecules each of **10b** and **11** in the unit cells. The single-crystal X-ray diffraction analysis of **10b** confirmed the expected planar geometry of the rigid tricyclic dithienophosphole, with the two thiophene moieties and the phosphole unit in an *anti* configuration (see Figure 1). The high degree of π conjugation is apparent in the short single bonds as well as in the elongated double bonds of the fused ring systems. However, the bond shortening/elongation is slightly more pronounced in **10b** than in **1a**[16a] presumably due to the presence of the electron-accepting silyl groups in **10b** and the oxygen substituent on the phosphorus atom. The high degree of π conjugation is further supported by the elongated bonds between the silicon atoms and the carbon atoms of the thiophene ring (Si1–C1: 1.864(3) Å, Si1A–C1A: 1.867(3) Å, Si2–C8: 1.867(2) Å, Si2A–C8A: 1.873(2) Å). The somewhat elongated C4–C5 (1.455(3) Å) and C4A–C5A (1.454(3) Å) bonds between the two thiophene units are in accordance with the enhanced electron-acceptor properties of the phosphorus center in **10b** compared with **1a**.[16a] Additional delocalization of the π-conjugated system through the phosphorus center should be possible in **10b** leading to elongation of the C4(A)–C5(A) bond as well as the aforementioned bond lengths of the dithieno ring system thus suggesting increased aromatic character in the phosphole subunit (vide infra). These structural features indicate that substitution of the phosphorus center can indeed have an effect on the degree of π conjugation, which is potentially interesting in terms of the optoelectronic properties of the material.

In the case of **11**, one of the molecules in the unit cell exhibits some disorder in the dithienophosphole ring unit and at one silyl group,[23] whereas the other molecule is somewhat disordered at one silyl group only allowing for discussion of some of the structural features of **11** in the solid state (Figure 2). Similar to the observations made for **1a**[16a] and **10b**, the high degree of π conjugation in the dithienophosphole system is apparent in the elongated double bonds and the shortened single bonds of the ring system, as well as the elongated bonds between the silicon atoms and the carbon atoms of the thiophene ring (Si1A–C1A: 1.874(3) Å: Si2A–C8A: 1.870(4) Å). The slightly elongated bond between the two thiophene units (C4A–C5A: 1.461(4) Å; cf. 1.440(2) Å for **1a**[16a]), which is comparable to that in **10b**, as well as the shortened P–C bonds, supports the electron-accepting nature of the phosphorus atom in **11**.

Reaction of **6** with the Lewis acid BH_3 (used as $BH_3{\cdot}SMe_2$) in dichloromethane at room temperature afforded the Lewis acid–base adduct **12** in quantitative yield.

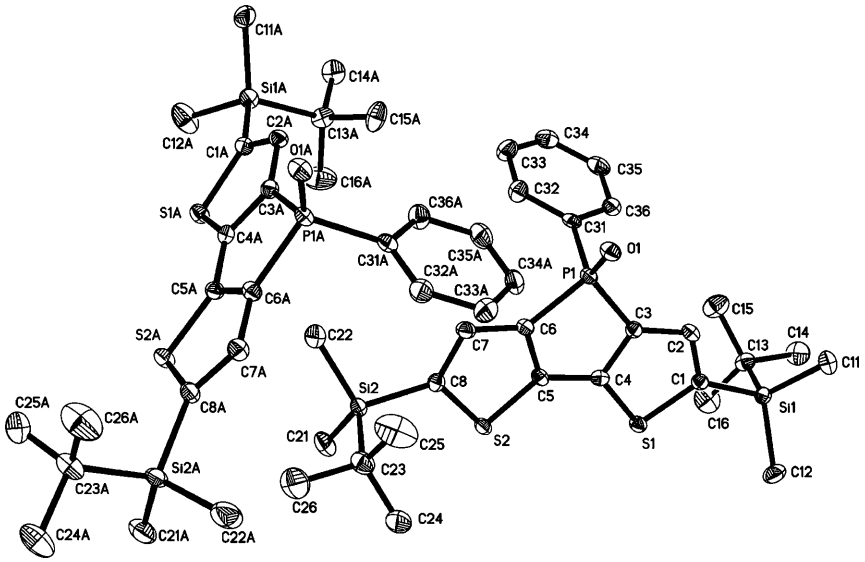

Figure 1. Molecular structure of **10b** (50% probability level) in the solid state. Hydrogen atoms are omitted for clarity. Selected bond lengths (Å): C1–C2: 1.380(3); C2–C3: 1.413(3); C3–C4: 1.385(3); C4–C5: 1.455(3); C5–C6: 1.380(3); C6–C7: 1.412(3); C7–C8: 1.378(3); P1–C3: 1.811(2); P1–C6: 1.812(2); P1–C31: 1.809(3); Si1–C1: 1.864(3); Si2–C8: 1.867(2).

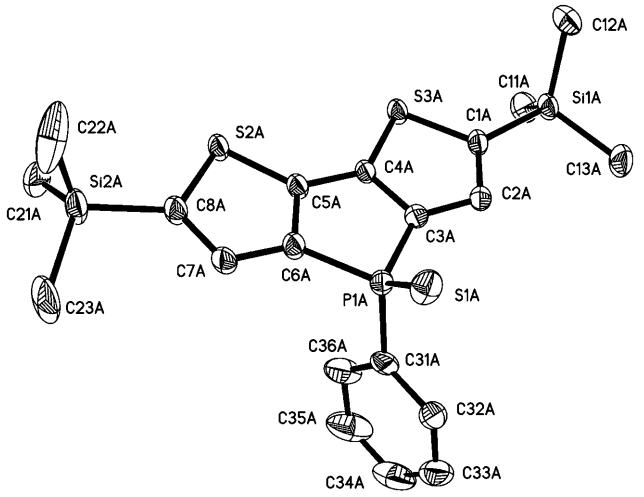

Figure 2. Molecular structure of **11** (50% probability level) in the solid state. Hydrogen atoms and the second, more disordered, molecule are omitted for clarity. Selected bond lengths (Å): C1A–C2A: 1.377(4); C2A–C3A: 1.406(4); C3A–C4A: 1.381(4); C4A–C5A: 1.461(4); C5A–C6A: 1.378(4); C6A–C7A: 1.413(4); C7A–C8A: 1.375(4); Si1A–C1A: 1.874(3); Si2A–C8A: 1.870(4); P1A–C3A: 1.804(3); P1A–C6A: 1.803(3); P1A–C31A 1.810(3).

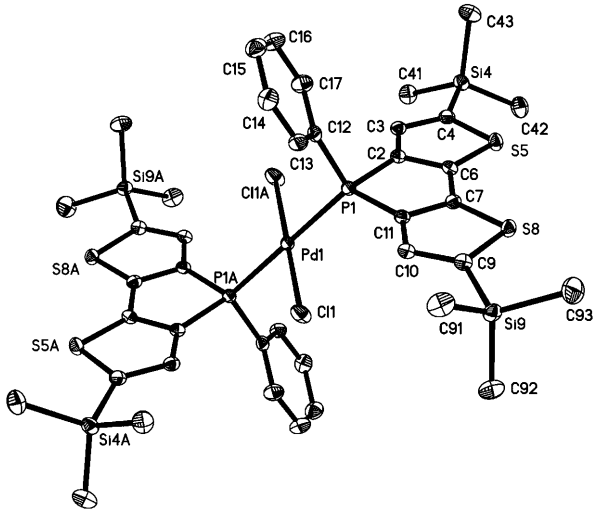

Figure 3. Molecular structure of **13** (50% probability level) in the solid state. Hydrogen atoms and three toluene solvent molecules are omitted for clarity. Selected bond lengths (Å): Pd1–Cl1: 2.3036(5); Pd1–P1: 2.3080(5); C2–C6; 1.382(3); C7–C11: 1.380(3); C6–C7: 1.448(3); C2–C3/C10–C11: 1.415(3); C3–C4: 1.373(3); C9–C10: 1.377(3); C4–Si4: 1.875(2); C9–Si9: 1.879(2); P1–C2: 1.809(2); P1–C11: 1.8183(2); P1–C12: 1.822(2).

Again, the ^{31}P NMR resonance is shifted downfield ($\delta^{31}P = 12.1$ ppm) as a result of an increase in the acceptor properties of the phosphorus center, but not as much as that observed for the phosphorus(v) species **10** and **11** in accordance with the electronic nature of the Lewis adduct.[16a] The ^{11}B NMR spectrum exhibits a resonance at $\delta = -39.4$ ppm that is typical of phosphane–borane adducts[24] and the ^{1}H and ^{13}C NMR data are comparable to related dithienophospholes.[16a]

In order to investigate the ligand properties of the dithienophosphole system, we reacted two equivalents of **6** with one equivalent of [Pd(cod)Cl_2] (cod = 1,5-cyclooctadiene) in $CHCl_3$ at room temperature. The ^{31}P NMR spectrum of **13** revealed the presence of two different species at $\delta^{31}P = 1.5$ and 8.9 ppm suggesting the generation of two isomers (*trans*/*cis*) in a ratio of 3:1. By comparison with related bisphosphane palladium complexes, the low-field resonance can be attributed to a *cis*-configured complex whereas the high-field species correlates to the *trans* isomer.[25,26] The ^{1}H NMR data are unexceptional, but the ^{13}C NMR data show a noteworthy feature: most of the signals in the ^{13}C NMR spectrum exhibit a pseudotriplet splitting due to coupling to two different phosphorus centers located on the same and the adjacent dithienophosphole ligand.

Orange-red crystals of **13** suitable for an X-ray diffraction study were obtained from a concentrated toluene solution at room temperature. Similar to an earlier observation,[26] the structural data revealed a *trans*-complex geometry (Figure 3), even though *cis*-[Pd(cod)Cl_2] was used as the starting material, supporting the NMR data for **13** in solution. Owing to an inversion center at the central palladium atom, the two dithienophosphole ligands exhibit an *anti* configuration (nearly C_{2h} symmetry) with a coplanar arrangement of the ring systems. The palladium atom exhibits a near-perfect square-planar geometry and the Pd–Cl (2.3036(5) Å) and Pd–P (2.3080(5) Å) bond lengths surprisingly are almost similar. Whereas in known palladium-phosphole complexes the Pd–Cl and Pd–P bonds usually differ significantly[25–28] for steric reasons, a combination of electronic and steric effects may cause the bond lengths in **13** to be similar. The phosphorus atom adopts a slightly distorted tetrahedral geometry similar to related phosphole complexes.[25–28] Consistent with the dithienophospholes **1a**,[16a] **10b**, and **11**, the lengths of the C–C bonds of the phosphole moiety show similar trends; that is, the C2–C6 (1.382(3) Å) and the C7–C11 bonds (1.380(3) Å) are again elongated whereas the C6–C7 bond (1.448(3) Å) is shortened. The same is true for the bond lengths of the thiophene subunits; the C2–C3/C10–C11 bonds of 1.415(3) Å each and the C3–C4/C9–C10 bonds of 1.373(3)/1.377(3) Å correspond to those of **1a**,[16a] **10b**, and **11**, which supports the expected degree of π conjugation in **13**. The relatively long exohedral C–Si bonds of 1.875(2) Å (C4–Si4) and 1.879(2) Å (C9–Si9) again suggest extension of the π system to the silicon atoms, supporting the importance of acceptor substituents in the optimized electronic structures of the dithienophospholes. The endohedral P–C bond lengths of 1.809(2) Å for P1–C2 and 1.8183(2) Å for P1–C11 correspond to those observed for **10b** and **11** and reflect the change in the electronic nature of the phosphorus atom now displaying a strong acceptor center.

Optoelectronic properties: Dithienophospholes **6–13** exhibit a strong blue photoluminescence. This feature has many potential applications since the detection of fluorescence is rapidly becoming the method of choice in materials science

and optoelectronics and also in medical and environmental studies.[29,30] Owing to its highly sensitive, selective, and safe nature it allows, for example, the observation of living processes and electronic transitions. Luminescence in materials can reflect the delocalization and polarization of the electronic structure.[31] Therefore, changing the electronic structure of a material should affect its luminescence properties. Any structural changes can easily be detected in the fluorescence phenomena and would allow dithienophospholes to be used as sensory materials once a library for different derivatives has been created.

For this reason we have investigated the photoluminescence (PL) properties of eight representative systems involving a σ^3,λ^3-phosphorus center (**6–9**), one of two different σ^4,λ^5-phosphorus centers (**10a**, **11**), a Lewis acid–base adduct (**12**), or a transition-metal-substituted phosphorus center (**13**). As expected, species with structurally different phosphorus centers have different maximum wavelengths for excitation (λ_{ex}) and emission (λ_{em}) reflecting the electronic nature of the respective systems. Surprisingly, the maximum wavelengths for emission from the σ^3,λ^3-phosphorus-containing systems **6–9** all appear at $\lambda_{em}=422$ nm, whereas the wavelengths for excitation/absorption are significantly affected by different substituents. As a result λ_{ex} experiences a redshift upon introduction of a *tert*-butyl group at the silyl centers ($\lambda_{ex}=364$ nm for **8**, $\lambda_{ex}=365$ nm for **9**; cf. $\lambda_{ex}=344$ nm for **6**) which is consistent with the stronger $+I$ effect of the *tert*-butyl unit compared with the methyl moiety. This effect is even more pronounced in **7** in which the *tert*-butyl group is connected directly to the phosphorus center with $\lambda_{ex}=372$ nm (see Table 1). Complete removal of the silyl functionalities, as in dithienophospholes **1a**,**b**, on the other hand, leads to a significant blueshift in the maximum wavelengths for excitation as well as emission (**1a**: $\lambda_{ex}=338$ nm, $\lambda_{em}=415$ nm; **1b**: $\lambda_{ex}=338$ nm, $\lambda_{em}=408$ nm),[16a] which reflects the effect of acceptor components present in the system.

Table 1. Optical and electrochemical data for **1a**,**b**, **6–13**, **15**, **16**, and **18**.

Compound	λ_{ex} [nm][a]	λ_{em} [nm][b]	$\lg(\varepsilon/\ dm^3 mol^{-1} cm^{-1})$	ϕ_{PL}[c]	E_{PA} [V][d]
1a	338	415	4.38	0.779	1.20
1b[e]	336	408	4.50	0.881	1.22
calcd	*334*		*(0.2)*[f]		
6	344	422	4.26	0.604	1.35
calcd	*350*		*(0.44)*[f]		
7	372	422	4.39	0.724	1.24
8	364	422	4.51	0.794	–
9	365	422	4.46	0.730	–
10a	374	460	4.09	0.556	1.59
calcd	*374*		*(0.34)*[f]		
11	374	460	4.00	0.556	1.55
calcd	*397*		*(0.1)*[f]		
12	355	432	4.10	0.545	1.54
calcd	*358*		*(0.41)*[f]		
13	384	470	4.03	0.614	1.42, 1.58
15	357	427	4.42	0.687	–
16	379	463	4.40	0.572	–
18	456, 502	555	–	–	–

[a] λ_{max} for excitation in CH_2Cl_2. [b] λ_{max} for emission in CH_2Cl_2. [c] Fluorescence quantum yield (±10%) relative to quinine sulfate (0.1 M H_2SO_4 solution); excitation at 365 nm. [d] Measured in CH_2Cl_2 versus SCE. [e] See ref. [16a]. [f] Relative intensity.

Oxidation of the phosphorus atom with oxygen or sulfur increases the electron-accepting ability of the phosphorus atom resulting in a redshift of about 30 nm for λ_{ex} and about 40 nm for λ_{em} (**10a**/**11**: $\lambda_{ex}=374$ nm, $\lambda_{em}=460$ nm). The phosphole–borane adduct **12** shows maximum wavelengths for excitation at 354 nm and emission at 432 nm, which lie between the values for the σ^3,λ^3 species **6** and the oxidized σ^4,λ^5 compounds **10a** and **11**, consistent with the electronic nature of the Lewis acid–base pair and as anticipated from ^{31}P NMR spectroscopy. The wavelength maxima for the palladium complex **13** show the strongest redshift ($\lambda_{ex}=384$ nm, $\lambda_{em}=470$ nm) which can be attributed to the electronic interactions between the dithienophosphole ligand and the transition-metal center. Note that photoluminescence is only significant when **13** is irradiated at the maximum excitation wavelength ($\lambda_{ex}=384$ nm). Irradiation at 365 nm results in an almost negligible emission at 470 nm indicating a very narrow window for the photoluminescence of **13**.

Owing to the similar nature of oxygen and sulfur, compounds **10a** and **11** exhibit similar λ_{ex} and λ_{em}. However, the relative intensities of their emissions are significantly different (ratio of ca. 8:1 for **10a**/**11**) suggesting that fluorescence is noticeably quenched by the soft sulfur substituent. This indicates that the relative emission intensities detected by fluorescence spectroscopy may well prove helpful to distinguish between closely related compounds. The relative emission intensities (with concentrations) of **6** and **10a–13** are shown in Figure 4. By using compound **11** as a standard, the intensity of the emission from **13** (at $\lambda_{ex}=384$ nm) and **6** is seen to be almost six times higher whereas compound **10a** shows much stronger fluorescence that amounts to approximately eight times the intensity of **11**. The borane adduct **12** exhibits the strongest emission intensity being almost twelve times stronger than that for **11**. Note also that the photolu-

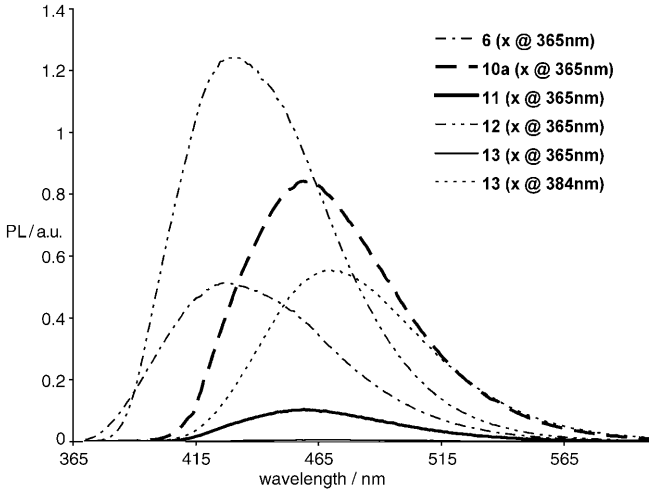

Figure 4. Fluorescence emission spectra of **6** ($c=5\times0^{-5}$ M), **10a** ($c=1\times10^{-4}$ M), **11** ($c=1\times10^{-4}$ M), **12** ($c=1\times10^{-4}$ M), and **13** ($c=3\times10^{-5}$ M) with the relative intensities shown.

minescence quantum yields of all the investigated dithienophosphole species are extraordinarily high ranging between 54 and almost 90% which is unprecedented for phospholes[1f] or dithieno systems.[9,12,14] This behavior is possibly related to the rigid structure of the anellated ring system which reduces the probability of internal conversions.

These results strongly underline the supposition that the dithienophosphole system is an excellent candidate for use as optoelectronic material because it allows its electronic properties to be fine-tuned in multiple ways to accommodate the needs of certain applications: Manipulation of the electronic nature of the phosphorus center affords the most significant shifts in the absorption and emission wavelengths allowing the luminescence properties of the material to be adjusted over a relatively broad range (~50 nm). In addition, functionalization of the thiophene unit, for example, as shown here with silyl groups, represents another valuable tool to further tune the luminescence properties of the system—other functional groups could also be considered. Very importantly, the optoelectronic properties can even be fine-tuned by variation of the substituents at the phosphorus and silicon centers. In this way only the maximum wavelength for excitation (λ_{ex}) can be tweaked to adjust the Stokes shift of the material selectively since the wavelength for emission (λ_{em}) remains unaffected in this case.

Theoretical calculations: To gain a deeper understanding of the effects that influence the electronic structure of the dithieno[3,2-*b*:2′,3′-*d*]phospholes investigated, we have carried out quantum chemical calculations. In order to study the substituent effects systematically we have considered not only the synthesized compounds, but we have also attached the substituents to the ring system **T** in a stepwise manner.

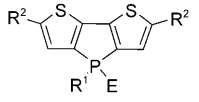

T

T1: R^1=R^2=H; E: lone pair
T2: R^1=Ph; R^2=H; E: lone pair
T3: R^1=H R^2=$SiMe_3$; E: lone pair
T4: R^1=Ph; R^2=$SiMe_3$; E: lone pair

The HOMO and LUMO of **T1** are shown in Figure 5 (top). Both orbitals can easily be derived from the frontier orbitals of both phosphole and thiophene and are also similar to the orbitals of dithieno[3,2-*b*:2′,3′-*d*]cyclopentadiene (**S2b**, E = CH_2) (Figure 5, bottom). The HOMO is an antibonding combination of the thiophene molecule's HOMOs, and at the phosphole ring, it is very similar to the phosphole molecule's HOMO. The LUMO is a bonding combination of the thiophene molecule's LUMOs, with some contribution from the σ^*_{PH}-MO, similar to the phosphole LUMO at the central five-membered ring. The fact that both frontier orbitals can easily be derived from the orbitals of the constituent rings shows that the π system is well delocalized over the entire molecule. Thus, none of the subunits of the ring system dominates the electronic structure and the dithieno[3,2-*b*:2′,3′-*d*]phosphole should be described as an entity. While the HOMO has a nodal plane through the phosphorus atom and its substituent, the LUMO has some contribution from the σ*(P–R_1) orbital, and it is clear that it will be affected by chemical modifications to this atom. The LUMO of **S2b** has a smaller contribution from the σ*(C–R_1) orbital than its phosphorus analogue **T1** (Figure 5). This orbital is responsible for the tuning of the optoelectronic properties that results from modification of the substituents at the phosphorus atom.

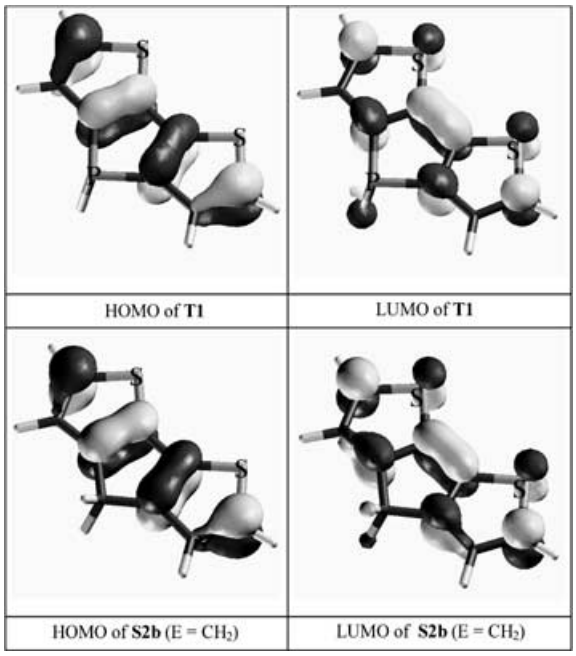

Figure 5. Frontier orbitals of the parent dithieno[3,2-*b*:2′,3′-*d*]phosphole (top) and dithieno[3,2-*b*:2′,3′-*d*]cyclopentadiene (bottom).

The calculated structural parameters match the available X-ray structural data closely. The data obtained for the parent dithieno[3,2-*b*:2′,3′-*d*]phosphole are in accordance with expectations. The bond lengths of the bithienyl framework are similar to those of dithieno[3,2-*b*:2′,3′-*d*]cyclopentadiene (**S2b**, E = CH_2), indicating that the replacement of the CH_2 group by a PH unit results in only small changes to the structure. In the C–C framework the formal single bonds in each ring shorten to 1.440 and 1.424 Å (cf. 1.459 and 1.430 Å for the phosphole and thiophene rings, respectively), while the formal double-bond lengths increase to 1.385 Å each (cf. 1.356 and 1.367 Å for the phosphole and the thiophene rings, respectively).

To assess the delocalization in the ring systems we have calculated the Bird indices (BI)[32] which are used to measure the aromaticity in the ring, as judged by the alternation of the bond lengths in all the **T1**–**T4** derivatives. The maximum value of this index is set to 100 (e.g., in the case of benzene in which there is no bond-length alternation). Phosphole itself has a low Bird index of 47, while the thiophene BI value is 68. The Bird indices are somewhat higher in the anellated system for both the phosphole (BI = 53) and

thiophene (BI = 71) rings, indicating that the delocalization is extended in the dithieno[3,2-*b*:2′,3′-*d*]phospholes in agreement with the previous conclusions obtained from the molecular orbitals. The Bird index of the cyclopentadienyl ring in **S2b** (E = CH_2) is lower than that of the phosphole ring (BI = 41), while it remains unaltered in the thienyl rings (BI = 72).

Phenyl substitution at the phosphorus atom of the phosphole ring results in negligible structural changes with the calculated bond lengths matching the X-ray data almost exactly.[16a] Silyl substitution at the thienyl rings also results in only small structural changes. The effect of oxo and thiono groups at the phosphorus atom is somewhat larger; the length of the C–C bond opposite the phosphorus atom in the five-membered ring is slightly lengthened upon oxidation of the phosphorus atom either by oxygen (e.g., 1.454 Å for **T1=O**) or sulfur (e.g., 1.451 Å for **T1=S**), while the exocyclic P–C bond lengths are shortened (e.g., 1.827 Å for **T1=O** and 1.829 Å for **T1=S**), increasing somewhat the aromatic character of the phosphole ring (e.g., **T1=O**: BI = 57; **T1=S**: BI = 56). (The increased bond order of the P–C bonds compensates the decrease in the bond order of the C–C bond.)

While the structural parameters of the substituted dithieno[3,2-*b*:2′,3′-*d*]phospholes investigated are similar, the time-dependent (TD)-DFT-calculated optoelectronic properties show a much larger variance. This is in accordance with the fact that substituents on the phosphorus atom have a direct effect on its contribution to the LUMO. In accordance with the involvement of the σ^*_{PH} orbital in the dithieno[3,2-*b*:2′,3′-*d*]phosphole LUMO, the calculated excitation energy of **T1** (324 nm) is lower than that of **S2b** (310 nm). Further substitution by phenyl (at the phosphorus atom) and by the trimethylsilyl groups lowers the excitation energy. An even larger effect is caused by oxygen or sulfur substitution at the phosphorus center; these substituents lower the LUMO energy considerably. The TD-DFT-calculated excitation energies show surprisingly good agreement with the observed band maxima for all compounds for which experimental data are available (see Table 1). Thus, such computations are extremely helpful in predicting the optoelectronic properties of dithieno[3,2-*b*:2′,3′-*d*]phospholes.

Synthesis of extended π-conjugated dithienophosphole systems: It would be of great advantage for future materials applications to be able to exploit the favorable properties possessed by macromolecules in terms of their processibility (i.e., their ability to form thin films) as recently shown by our group.[16a] For this reason, the intriguing results obtained from the investigation of the optoelectronic properties of the dithienophosphole monomers/model compounds stimulated us to further explore the incorporation of the dithienophosphole moiety into extended oligomeric or polymeric materials. In this context, the synthesis of materials with an exclusively π-conjugated backbone is of particular interest as the resulting oligomers/polymers might be expected to exhibit semiconducting properties that would open up even greater possibilities for applications in molecular electronics.

In order to probe the access to the desired extended π-conjugated systems we initially targeted a synthetic protocol that involves Stille coupling, which has successfully been utilized in the synthesis of thiophene-containing polymers before.[33] The required tin functionalization of the monomers was achieved by reaction of 3,3′,5,5′-tetrabromo-2,2′-bithiophene (**3**) with two equivalents each of *n*BuLi and tributyltin chloride in THF at −78 °C in a similar procedure to that used in the synthesis of silyl-substituted species **4** and **5**. 3,3′-Dibromo-5,5′-bis(tributyltin)-2,2′-bithiophene (**14**) was obtained in 88% yield and can be treated with another two equivalents of *n*BuLi in Et_2O at −78 °C in the presence of a five-fold excess of TMEDA. The tin-functionalized dithienophosphole **15** was obtained in fair yields (ca. 65%) after addition of $PhPCl_2$ and subsequent filtration through neutral alumina. Note, that one of the major byproducts of this reaction is tetrabutyltin, which is presumably generated by nucleophilic attack by *n*BuLi at the tin centers of **14**. This side-reaction can be suppressed to some extent by the addition of TMEDA, which coordinates to the tin centers and thus reduces the access of *n*BuLi. This observation, however, underlines the leaving-group character of the tin group and could be beneficial for the generation of extended π-conjugated moieties. The dithienophosphole **15** exhibits a ^{31}P NMR chemical shift at $\delta = -28.0$ ppm, which is in the same range as those observed for the silyl-functionalized congeners **6**, **8**, and **9**. The same is true for the ^{1}H and ^{13}C NMR data of the tin-functionalized dithienophosphole **15**.

However, the Stille-coupling protocol generally requires a palladium catalyst, but the dithienophosphole system itself is a suitable ligand for a palladium center (see **13**) that could potentially poison the catalyst and inhibit the catalytic process. We therefore anticipated that it would be necessary to protect the phosphorus center of the dithienophosphole in order to achieve the desired cross-coupling reaction. We decided to test the corresponding phosphole oxide **16**, which was synthesized by a similar procedure to that described for the corresponding silyl-functionalized dithienophospholes **10a**,**b**. The observed trend in the multinuclear NMR data of **16** corresponds to that of its silyl relatives with a ^{31}P NMR chemical shift at $\delta^{31}P = 14.7$ ppm, which is slightly shifted upfield relative to that of **10a**,**b**. The same is true for the optoelectronic properties of **15** and **16**, which have wavelength maxima that are almost similar to those of the silyl-functionalized derivatives with a significant redshift of $\Delta\lambda_{ex} \approx 20$ nm and $\Delta\lambda_{em} \approx 40$ nm for **16** relative to **15** ($\lambda_{ex} = 357$ nm; $\lambda_{em} = 427$ nm, see Table 1).

Preliminary cross-coupling reactions following a typical Stille protocol were then performed by treating **16** in THF or *N*-methylpyrrolidinone (NMP) with a mixture of [Pd(PPh_3)$_4$] and CuI as catalysts using 1,4-diiodo-2,5-bis(octyloxy)benzene **17** as the aryl halide component (Scheme 3). The alkyloxy substituents of the diiodobenzene were anticipated to aid the necessary solubility of the targeted materials. In the course of our work NMP was found to

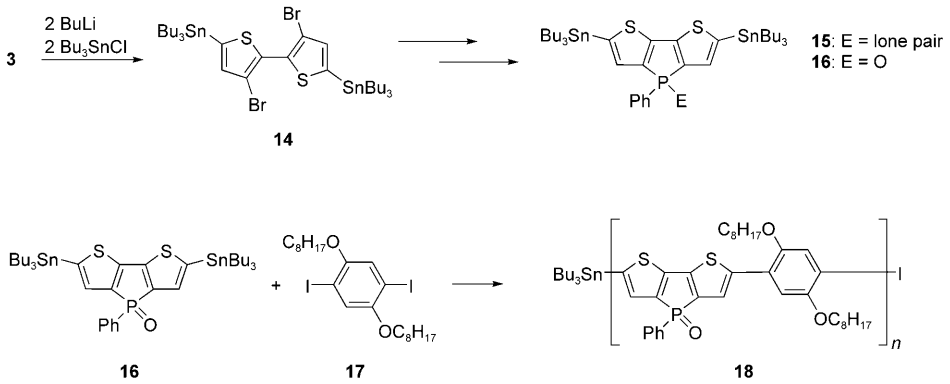

Scheme 3. Synthesis and polymerization of tin-functionalized dithieno[3,2-*b*:2′,3′-*d*]phospholes.

be the solvent of choice for these experiments owing to its high boiling point which allowed the cross-coupling reaction to be performed at around 200 °C, which is apparently essential for the formation of longer chains. After two days, a reddish-brown material was obtained after evaporation of the solvent and precipitation from THF in hexane. The ^{31}P NMR spectrum of **18** revealed one very broad resonance at $\delta^{31}P \sim 14$ ppm. This indicated the presence of only one phosphorus species and correlates well with a dithienophosphole oxide. The formation of the desired product is further supported by the ^{1}H and ^{13}C NMR spectra of **18** which exhibit (broad) resonances due to the aryl and the alkyloxy moieties. Owing to the reduced solubility of the extended π-conjugated material in THF, we were unable to obtain an exact molecular weight for **18** by GPC analysis, but the formation of dithienophosphole-containing chains with a broad molecular weight distribution is supported by the data. The success of the cross-coupling step is further supported by the optoelectronic properties of the material (see Figure 6). The

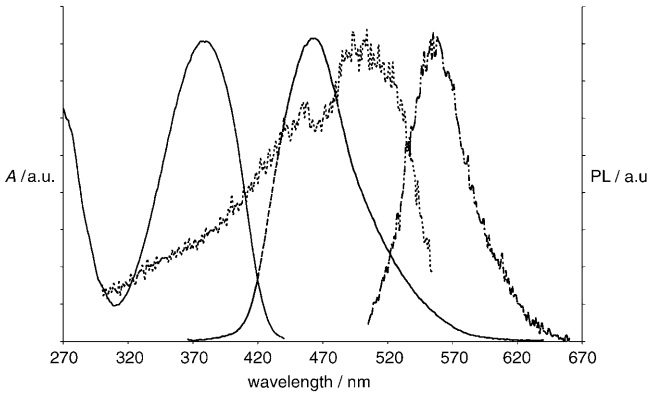

Figure 6. Normalized fluorescence spectra (excitation and emission) of **15** (– – –) and **18** (•••••) in CH_2Cl_2.

strongly extended π conjugation of **18** is evident in a very significant redshift of the maximum wavelength for excitation ($\lambda_{ex} = 456$, 502 nm) and an emission at $\lambda_{em} = 555$ nm in the yellow-green region of the optical spectrum (cf. **16**: $\lambda_{ex} =$ 379 nm; $\lambda_{em} = 463$ nm). These preliminary findings suggest that extended π-conjugated dithienophosphole materials are accessible by this route and therefore optimization of the reaction conditions is currently undergoing detailed investigation.

Conclusions

In conclusion, we have synthesized a novel class of phosphorus-based materials that are potentially very useful in molecular electronics. The very flexible protocol for the synthesis of the dithieno[3,2-*b*:2′,3′-*d*]phosphole system allows access to a wide variety of differently functionalized species with intriguing optoelectronic properties with respect to wavelength and intensity. Chemically facile modifications to the central phosphorus atom allow the electronic structure of the system to be tuned very efficiently. Further fine-tuning can be accomplished by the proper choice of exocyclic substituents, which allows, for example, selective manipulation of the absorption properties of the material while the emission properties remain unaffected thus modifying the Stokes shift in an efficient way. The versatile tunability of the material opens up a multitude of potential applications for dithienophospholes in molecular electronics, for example, as blue-light emitter material in OLEDs/PLEDs, as sensory material, and as organic transistor material (OTFT).

The theoretical investigations of the dithieno[3,2-*b*:2′,3′-*d*]phosphole system have shown that this system has a unique electronic structure that is derived from bithiophene, but which is significantly influenced by the phosphorus atom. Furthermore, the results emphasize the fact that structural changes to the system are governed by the occupied orbitals. While these remain more or less unchanged, the optical properties can be significantly influenced by the unoccupied orbitals, particularly by the LUMO, which is sensitive to substitution at the phosphorus center. Following from this, several properties of the system can be simulated very efficiently. Especially noteworthy is the ability of the time-dependent DFT calculations to match the experimentally observed UV absorptions almost perfectly. Hence this type of theoretical calculation can be used to predict the optoelectronic properties of unknown dithienophosphole species, resulting in the "stream-lined" design of dithienophosphole materials for use in molecular electronics.

Our initial results obtained by using the Stille cross-coupling protocol clearly indicate that it should be possible to generate long chain, exclusively π-conjugated dithienophosphole oligomers/polymers by this route. However, further studies need to be performed to find the optimized reaction conditions for this cross-coupling step. Functionalities

that enhance the solubility of the material are required if the targeted polymeric materials are to be analyzed comprehensively. Good solubility (i.e., processability) is as important for prospective applications in organic or polymer-based light-emitting diodes (OLED/PLED) as a broad molecular weight distribution. We are therefore currently looking to vary the aryl halide component and other solubilizing groups as well as investigating the Suzuki cross-coupling protocol as an alternative way to access these intriguing materials.

Experimental Section

Calculations: Theoretical calculations were carried out at the B3LYP/6-31G* level by using the Gaussian 98 suite of programs:[34] This level of theory has provided satisfactory results for the phosphole–thiophene oligomers before.[1f] The geometries were fully optimized and second derivatives were calculated for the resulting structures. Only positive eigenvalues of the Hessian matrix were obtained, proving that all the structures obtained are real minima on the potential-energy hypersurface. The vertical excitation energies were calculated for the optimized structures by the time-dependent (TD) density functional method by using the B3LYP functional and the 6-31G* basis set.

The Bird index was calculated according to the original procedure of Bird.[32] However, when the Gordy equation[35] was used to obtain bond orders from the calculated bond lengths we used the "a" and "b" constants developed from the B3LYP/6-31G* optimized single- and double-bonded molecules (e.g., for the C–C bond we used ethane and ethylene with bond orders of one and two, respectively).

General procedures: Reactions were carried out in dry glassware and under inert atmosphere of purified argon by using Schlenk techniques. Solvents were dried over appropriate drying agents and then distilled. *n*BuLi (2.5 M in hexane), H_2O_2 (30% in H_2O), sulfur, $BH_3{\cdot}SMe_2$ (1 M in CH_2Cl_2), and *t*BuMe$_2$SiCl were used as received. Liquid reagents ($PhPCl_2$, Bu_3SnCl, and TMEDA) were freshly distilled prior to use. 3,3′,5,5′-Tetrabromo-2,2′-bithiophene (**3**),[36] 5,5′-bis(trimethylsilyl)-3,3′-dibromo-2,2′-bithiophene (**4**),[9a] $RPCl_2$ (R = *t*Bu[37] and 4-*t*BuC$_6$H$_4$[38]), [Pd(cod)Cl$_2$],[39] and 1,4-diiodo-2,5-bis(octyloxy)benzene (**18**)[40] were prepared by methods reported in the literature. ^{1}H, ^{13}C, ^{31}P, and ^{11}B NMR spectra were recorded with a Bruker DRX 400, Varian Mercury 200 or Unity 500 MHz-spectrometer. Chemical shifts are referenced to external 85% H_3PO_4 (^{31}P), $BF_3{\cdot}Et_2O$ (^{11}B) or TMS (^{13}C, ^{1}H). Electron ionization (70 eV) mass spectra were recorded with a Finnigan 8230 spectrometer. Elemental analyses were performed by the Microanalytical Laboratory of the Institut für Anorganische und Analytische Chemie, Johannes Gutenberg-Universität, Mainz. Crystal data and details of the data collection are provided in Table 2. Diffraction data for **10a** and **11** were collected with a Bruker SMART D8 goniometer with an APEX CCD detector and for **13** on a Nonius KappaCCD. The structures were solved by direct methods (SHELXTL) and refined on F^2 by full-matrix least-squares techniques. Hydrogen atoms were included by using a riding model.

CCDC 263187 (**10b**), 263186 (**11**), and 262991 (**13**) contain the supplementary crystallographic data for this paper. These data can be obtained free of charge from the Cambridge Crystallographic Data Centre via www.ccdc.cam.ac.uk/data_request/cif.

Table 2. Crystal data and structure refinement for **10b**, **11**, and **13**.[a]

	10b	**11**	**13·3C$_7$H$_8$**
formula	$C_{26}H_{37}OPS_2Si_2$	$C_{20}H_{25}PS_3Si_2$	$C_{40}H_{50}Cl_2P_2PdS_4Si_4{\cdot}3C_7H_8$
M_r	516.83	448.73	1287.04
T [K]	110(2)	110(2)	123(2)
λ [Å]	0.71073	0.71073	0.71073
crystal system	monoclinic	triclinic	triclinic
space group	$P(2)1/c$ (no.14)	$P\bar{1}$ (no.2)	$P\bar{1}$ (no.2)
a [Å]	14.411(5)	10.839(2)	8.6369(2)
b [Å]	12.392(4)	11.454(2)	12.7335(3)
c [Å]	32.359(11)	19.428(4)	15.2681(4)
α [°]	90	96.41(3)	99.497(1)
β [°]	97.101(9)	94.33(3)	99.985(1)
γ [°]	90	91.16(3)	94.185(1)
V [Å^3]	5734(4)	2389.2(8)	1622.11(7)
ρ_{calcd} [Mg m^{-3}]	1.197	1.248	1.318
Z	8	4	1
μ [mm^{-1}]	0.342	0.481	0.657
F(000)	2208	944	670
crystal size [mm^3]	0.41×0.37×0.13	0.44×0.17×0.06	0.50×0.40×0.30
θ range [°]	1.27–27.60	1.06–28.38	2.75–25.00
index ranges	$-18\le h\le 18$	$-14\le h\le 14$	$-9\le h\le 10$
	$-12\le k\le 16$	$-15\le k\le 15$	$-15\le k\le 15$
	$-41\le l\le 42$	$-25\le l\le 25$	$-18\le l\le 18$
reflections collected	43144	30361	19257
independent reflections	13228 (R(int) = 0.0515)	11887 (R(int) = 0.0434)	5709 (R(int) = 0.0317)
completeness to θ [°]	27.60 (99.6%)	28.38 (99.2%)	25.00 (99.8%)
absorption correction	empirical	empirical	none
max./min. transmission	0.959/0.937	0.9717/0.8163	–
data/restraints/parameters	13228/0/577	11887/72/469	5709/60/322
GOF on F^2	1.047	1.037	1.060
final R indices [$I>2\sigma(I)$]	R_1 = 0.0478, wR_2 = 0.1124	R_1 = 0.0601, wR_2 = 0.1487	R_1 = 0.0270, wR_2 = 0.0704
R indices (all data)	R_1 = 0.0683, wR_2 = 0.1261	R_1 = 0.0912, wR_2 = 0.1673	R_1 = 0.0328, wR_2 = 0.0725
largest diff. peak/hole [e Å^{-3}]	0.518/−0.316	1.158/−0.921	1.047/−0.688

[a] The refinement method was full-matrix least-squares on F^2 for all three compounds.

Synthesis of 5: *n*BuLi (8 mL, 20 mmol) was added dropwise to a solution of **3** (4.82 g, 10 mmol) in THF (100 mL) at −78 °C. The solution was stirred for 15 min at −78 °C and *tert*-butyldimethylsilyl chloride (3.01 g, 20 mmol) dissolved in THF (10 mL) was added dropwise to the reaction mixture at that temperature. The reaction mixture was allowed to warm slowly to room temperature and the solvent was subsequently removed under vacuum. The residue was taken up in pentane (ca. 60 mL) and filtered through neutral alumina. Evaporation of the solvent under vacuum provided **5** as beige solid (5.1 g, 93% yield).

^{1}H NMR (500 MHz, $CDCl_3$): δ = 7.15 (s; Ar-H), 0.95 (s, 18H; Si-*t*Bu), 0.31 ppm (s, 12H; $SiMe_3$); ^{13}C{^{1}H} NMR (125.7 MHz, $CDCl_3$): δ = 140.7 (s; Ar-Ar), 137.0 (s; Ar-H), 134.2 (s; Ar-Si), 112.8 (s; Ar-Br), 26.3 (s; SiC(CH_3)$_3$), 16.0 (s; Si*C*(CH$_3$)$_3$), −5.2 ppm (s; $SiMe_2$); MS (70 eV, EI): *m*/*z* (%): 552 (30) [M^+], 495 (100) [$M^+-C_4H_9$], 73 (25) [$SiMe_3^+$].

Synthesis of 6 and 7: *n*BuLi (4 mL, 10 mmol) was added dropwise to a solution of **4** (2.34 g, 5 mmol) in Et_2O (50 mL) at −78 °C. The solution was stirred for 1 h before the temperature was raised to approximately −30 °C. Subsequently, $RPCl_2$ (R = Ph: 0.90 g, 5 mmol; R = *t*Bu: 0.80 g, 5 mmol), dissolved in Et_2O (5 mL), was added slowly to the reaction mixture which was allowed to warm quickly to room temperature. The solvent was then removed under vacuum, and the residue taken up in *n*-hexane (ca. 50 mL) and filtered through neutral alumina to remove LiCl and some brown impurities. The filtrate was evaporated to dryness and **6**

and **7** were obtained as off-white solids (R = Ph: 1.50 g, 72% yield; R = *t*Bu: 1.43 g, 72% yield).

Compound **6**: $^{31}P\{^1H\}$ NMR (162 MHz, $CDCl_3$): $\delta = -25.0$ ppm; ^1H NMR (400 MHz, $CDCl_3$): $\delta = 7.34$ (br, 2H; *o*-Ph), 7.26 (br, 2H; *m*-Ph), 7.25 (br, 1H; *p*-Ph), 7.20 (s, 2H; Ar-H), 0.30 ppm (s, 18H; $Si(CH_3)_3$); $^{13}C\{^1H\}$ NMR (100.6 MHz, $CDCl_3$): $\delta = 148.6$ (d, $^2J(C,P) = 9.6$ Hz; Ar), 146.7 (br; Ar), 142.6 (d, $J(C,P) = 2.1$ Hz; Ar), 133.9 (d, $^1J(C,P) = 15.5$ Hz; *ipso*-Ph), 133.0 (d, $^2J(C,P) = 18.3$ Hz; *o*-Ar), 132.4 (d, $^2J(C,P) = 20.3$ Hz; *o*-Ar), 129.0 (s; *p*-Ph), 128.5 (d, $^3J(C,P) = 7.8$ Hz; *m*-Ph), −0.2 ppm (s; SiC_3); MS (70 eV, EI): *m/z* (%): 416 (80) [M^+], 73 (100) [$SiMe_3^+$]; elemental analysis calcd (%) for $C_{20}H_{25}PS_2Si_2$ (416.7): C 57.65, H 6.05, S 15.39; found: C 57.68, H 5.93, S 15.40.

Compound **7**: $^{31}P\{^1H\}$ NMR (162 MHz, $CDCl_3$): $\delta = 0.3$ ppm; ^1H NMR (400 MHz, $CDCl_3$): $\delta = 7.16$ (s, 2H; Ar-H), 1.03 (d, $^3J(H,P) = 13.7$ Hz, 9H; $C(CH_3)_3$), 0.31 ppm (s, 18H; $Si(CH_3)_3$); $^{13}C\{^1H\}$ NMR (100.6 MHz, $CDCl_3$): $\delta = 147.3$ (d, $^2J(C,P) = 15.9$ Hz; Ar), 147.0 (d, $^1J(C,P) = 35.4$ Hz; Ar), 141.6 (d, $J(C,P) = 3.7$ Hz; Ar), 133.3 (d, $^2J(C,P) = 16.4$ Hz; *o*-Ar), 32.3 (d, $^1J(C,P) = 12.4$ Hz; CMe_3), 27.5 (d, $^2J(C,P) = 14.3$ Hz; $C(CH_3)_3$), −0.1 ppm (s, SiC_3); elemental analysis calcd (%) for $C_{20}H_{25}PS_2Si_2$ (396.7): C 54.50, H 7.37, S 16.17; found: C 55.80, H 7.60, S 15.78.

Synthesis of 8 and 9: *n*BuLi (4 mL, 10 mmol) was added dropwise to a solution of **5** (2.78 g, 5 mmol) and TMEDA (1.51 mL, 10 mmol) in Et_2O (50 mL) at −78 °C. The solution was stirred for 1 h before the temperature was raised to ca. −30 °C. Subsequently, $RPCl_2$ (R = Ph: 0.90 g, 5 mmol; R = 4-*t*BuPh: 1.18 g, 5 mmol), dissolved in Et_2O (10 mL), was added slowly to the reaction mixture and the resulting mixture was allowed to warm quickly to room temperature. The solvent was then removed under vacuum, the residue taken up in pentane (ca. 60 mL) and filtered to remove LiCl. The filtrate was concentrated and left to crystallize at −30 °C. Compounds **8** and **9** were obtained as white amorphous solids (**8**: 2.0 g, 81% yield; **9**: 2.2 g, 78% yield).

Compound **8**: $^{31}P\{^1H\}$ NMR (80.9 MHz, $CDCl_3$): $\delta = -27.4$ ppm; ^1H NMR (500 MHz, $CDCl_3$): $\delta = 7.38$ (m, 2H; *o*-Ph), 7.30 (m, 3H; Ph-H), 7.26 (s, 2H; Ar-H), 0.94 (s, 18H; Si-*t*Bu), 0.32 (s, 6H; $SiMe_2$), 0.31 ppm (s, 6H; $SiMe_2$); $^{13}C\{^1H\}$ NMR (125.7 MHz, $CDCl_3$): $\delta = 148.7$ (d, $^1J(C,P) = 9.7$ Hz; *ipso*-Ar), 147.0 (d, $J(C,P) = 3.2$ Hz; Ar), 139.8 (d, $J(C,P) = 4.3$ Hz; Ar), 134.3 (d, $^2J(C,P) = 18.3$ Hz; *o*-Ar), 134.2 (d, $^1J(C,P) = 15.0$ Hz; *ipso*-Ph), 132.5 (d, $^2J(C,P) = 20.4$ Hz; *o*-Ar), 129.1 (s; *p*-Ph), 128.5 (d, $^3J(C,P) = 8.6$ Hz; *m*-Ph), 26.4 (s; $SiC(CH_3)_3$), 17.0 (s; $SiC(CH_3)_3$), −4.9 ppm (s; $SiMe_2$); elemental analysis calcd (%) for $C_{26}H_{37}PS_2Si_2$ (500.9): C 62.35, H 7.45, S 12.80; found: C 62.75, H 7.28, S 12.76.

Compound **9**: $^{31}P\{^1H\}$ NMR (80.9 MHz, $CDCl_3$): $\delta = -28.2$ ppm; ^1H NMR (500 MHz, $CDCl_3$): $\delta = 7.30$ (br, 2H; Ar-H), 7.27 (br, 2H; Ar-H), 7.24 (br, 2H; Ar-H), 1.26 (s, 9H; $C(CH_3)_3$), 0.92 (s, 18H; Si-*t*Bu), 0.29 (s, 6H; $SiMe_2$), 0.28 ppm (s, 6H; $SiMe_2$); $^{13}C\{^1H\}$ NMR (125.7 MHz, $CDCl_3$): $\delta = 152.3$ (s; *p*-Ar), 148.8 (d, $J(C,P) = 10.7$ Hz; Ar), 146.8 (d, $J(C,P) = 2.1$ Hz; Ar), 139.5 (d, $J(C,P) = 4.3$ Hz; Ar), 134.5 (d, $^2J(C,P) = 18.3$ Hz; *o*-Ar), 132.3 (d, $^2J(C,P) = 21.5$ Hz; *o*-Ar), 130.4 (d, $^1J(C,P) = 14.0$ Hz; *ipso*-Ar), 125.7 (d, $^3J(C,P) = 6.4$ Hz; *m*-Ar), 34.1 (s; CMe_3), 31.2 (s; $C(CH_3)_3$), 26.4 (s; $SiC(CH_3)_3$), 17.0 (s; $SiCMe_3$), −4.8 (s; SiMe), −4.9 ppm (s; SiMe); elemental analysis calcd (%) for $C_{30}H_{45}PS_2Si_2$ (557.0): C 64.70, H 8.14, S 11.51; found: C 65.03, H 8.96, S 10.76.

Synthesis of 10: Hydrogen peroxide (0.5 g, 3.3 mmol, 30% solution in H_2O) was added to a solution of **6** (1.25 g, 3 mmol) or **8** (1.50 g, 3 mmol) in THF (20 mL) at room temperature. The reaction mixture was stirred for 16 h. Subsequently, all volatile materials were removed under vacuum and the residue taken up in warm hexane (10 mL). Slow evaporation of the solvent provided **10a** as light yellow crystals and **10b** as colorless crystals (**10a**: 1.23 g, 95% yield; **10b**: 1.50 g, 97% yield).

Compound **10a**: $^{31}P\{^1H\}$ NMR (162.0 MHz, $CDCl_3$): $\delta = 17.2$ ppm; ^1H NMR (400 MHz, $CDCl_3$): $\delta = 7.73$ (dd, $^3J(H,P) = 13.4$, $^3J(H,H) = 7.4$ Hz, 2H; *o*-Ph), 7.50 (td, $^3J(H,H) = 7.4$, $^4J(C,P) = 2.0$ Hz, 1H; *p*-Ph), 7.40 (td, $^3J(H,H) = 7.8$, $^3J(H,P) = 3.1$ Hz, 2H; m-Ph), 7.16 (d, $^2J(H,P) = 2.1$ Hz, 2H; Ar-H), 0.28 ppm (s, 18H; $Si(CH_3)_3$); $^{13}C\{^1H\}$ NMR (100.6 MHz, $CDCl_3$): $\delta = 150.6$ (d, $J(C,P) = 24.9$ Hz; Ar), 145.5 (d, $J(C,P) = 11.0$ Hz; Ar), 140.7 (d, $^1J(C,P) = 108.6$ Hz; *ipso*-Ar), 132.1 (s; *p*-Ph), 132.0 (d, $^2J(C,P) = 13.0$ Hz; *o*-Ar), 130.8 (d, $^3J(C,P) = 11.4$ Hz; *m*-Ph), 129.9 (d, $^1J(C,P) = 107.5$ Hz; *ipso*-Ph), 128.6 (d, $^2J(C,P) = 13.0$ Hz; *o*-Ar), −0.3 ppm (s; SiC_3); MS (70 eV, EI): *m/z* (%): 432 (100) [M^+], 417 (55) [M^+−Me], 73 (40) [$SiMe_3^+$]; elemental analysis calcd (%) for $C_{20}H_{25}OPS_2Si_2$ (432.7): C 55.52, H 5.82, S 14.82; found: C 55.63, H 5.82, S 15.51.

Compound **10b**: $^{31}P\{^1H\}$ NMR (80.9 MHz, $CDCl_3$): $\delta = 14.9$ ppm; ^1H NMR (400 MHz, $CDCl_3$): $\delta = 7.67$ (dd, $^3J(H,P) = 13.5$, $^3J(H,H) = 7.5$ Hz, 2H; *o*-Ph), 7.45 (td, $^3J(H,H) = 7.5$, $^4J(C,P) = 1.9$ Hz, 1H; *p*-Ph), 7.36 (td, $^3J(H,H) = 7.8$, $^3J(H,P) = 3.3$ Hz, 2H; *m*-Ph), 7.12 (d, $^2J(H,P) = 2.2$ Hz, 2H; Ar-H), 0.83 (s, 18H; Si-*t*Bu), 0.20 (s, 6H; $SiMe_2$), 0.19 ppm (s, 6H; $SiMe_2$); $^{13}C\{^1H\}$ NMR (100.6 MHz, $CDCl_3$): $\delta = 150.9$ (d, $J(C,P) = 23.7$ Hz; Ar), 142.8 (d, $J(C,P) = 10.7$ Hz; Ar), 139.5 (d, $^1J(C,P) = 108.3$ Hz; *ipso*-Ar), 133.2 (d, $^2J(C,P) = 13.7$ Hz; *o*-Ar), 132.2 (d, $^4J(C,P) = 3.8$ Hz; *p*-Ph), 130.9 (d, $J(C,P) = 11.4$ Hz; *m*-Ar), 130.1 (d, $^1J(C,P) = 105.3$ Hz; *ipso*-Ph), 128.7 (d, $^2J(C,P) = 13.7$ Hz; *o*-Ar), 26.3 (s; $SiC(CH_3)_3$), 16.9 (s; $SiC(CH_3)_3$), −4.8 (s; SiMe), −4.9 ppm (s; SiMe); elemental analysis calcd (%) for $C_{26}H_{37}OPS_2Si_2$ (516.9): C 60.42, H 7.11, S 12.41; found: C 60.73, H 7.13, S 12.85.

Synthesis of 11: Elemental sulfur (100 mg, 3.1 mmol) was added to a solution of **6** (1.25 g, 3 mmol) in THF (20 mL) at room temperature and the reaction mixture was stirred for 16 h. Subsequently, the solvent was removed under vacuum and the residue taken up in warm hexane (10 mL). Slow evaporation of the solvent provided **11** as yellow crystals (1.24 g, 92% yield).

$^{31}P\{^1H\}$ NMR (162.0 MHz, $CDCl_3$): $\delta = 23.6$ ppm; ^1H NMR (400 MHz, $CDCl_3$): $\delta = 7.78$ (br, 2H; *o*-Ph), 7.47 (br, 1H; *p*-Ph), 7.38 (br, 2H; *m*-Ph), 7.17 (d, $^2J(H,P) = 2.3$ Hz, 2H; Ar-H), 0.28 ppm (s, 18H; $Si(CH_3)_3$); $^{13}C\{^1H\}$ NMR (100.6 MHz, $CDCl_3$): $\delta = 148.9$ (d, $J(C,P) = 21.1$ Hz; Ar), 145.9 (d, $J(C,P) = 11.1$ Hz; Ar), 143.2 (d, $^1J(C,P) = 90.8$ Hz; *ipso*-Ar), 131.8 (d, $^4J(C,P) = 3.2$ Hz; *p*-Ph), 131.3 (d, $^2J(C,P) = 14.1$ Hz; *o*-Ar), 130.7 (d, $^2J(C,P) = 12.4$ Hz; *o*-Ar), 129.9 (d, $^1J(C,P) = 84.0$ Hz; *ipso*-Ph), 128.6 (d, $^3J(C,P) = 13.4$ Hz; *m*-Ph), −0.4 ppm (s; SiC_3); MS (70 eV, EI): *m/z* (%): 448 (100) [M^+], 433 (10) [M^+−Me], 371 (85) [M^+−Ph], 73 (30) [$SiMe_3^+$]; elemental analysis calcd (%) for $C_{20}H_{25}PS_3Si_2$ (448.8): C 53.53, H 5.62, S 21.44; found: C 53.52, H 5.52, S 21.09.

Synthesis of 12: $BH_3{\cdot}SMe_2$ (3.3 mL, 3.3 mmol) was added to a solution of **6** (1.25 g, 3 mmol) in CH_2Cl_2 (20 mL) at room temperature and the reaction mixture was stirred for 1 h. Subsequently, all volatile materials were removed under vacuum to provide **12** as yellowish crystals (1.28 g, 99% yield).

$^{31}P\{^1H\}$ NMR (162.0 MHz, $CDCl_3$): $\delta = 12.1$ ppm (br); $^{11}B\{^1H\}$ NMR (128.4 MHz, $CDCl_3$): $\delta = -39.4$ ppm; ^1H NMR (400 MHz, $CDCl_3$): $\delta = 7.60$ (dd, $^3J(H,P) = 11.7$, $^3J(H,H) = 7.5$ Hz, 2H; *o*-Ph), 7.50 (brt, $^3J(H,H) = 7.5$ Hz, 1H; *p*-Ph), 7.36 (brt, $^3J(H,H) = 7.5$ Hz, 2H; *m*-Ph), 7.17 (d, $^3J(H,P) = 1.1$ Hz, 2H; Ar-H), 1.1 (very broad, 3H; BH_3), 0.30 ppm (s, 18H; $Si(CH_3)_3$); $^{13}C\{^1H\}$ NMR (100.6 MHz, $CDCl_3$): $\delta = 149.7$ (d, $J(C,P) = 11.5$ Hz; Ar), 145.4 (d, $J(C,P) = 8.7$ Hz; Ar), 140.5 (d, $^1J(C,P) = 59.6$ Hz; *ipso*-Ar), 132.1 (d, $^2J(C,P) = 14.3$ Hz; *o*-Ar), 131.8 (d, $^2J(C,P) = 10.9$ Hz; *o*-Ar), 131.6 (s; p-Ph), 130.1 (d, $^1J(C,P) = 94.1$ Hz; *ipso*-Ar), 128.8 (d, $^3J(C,P) = 10.6$ Hz; *m*-Ph), −0.3 ppm (s; SiC_3); MS (70 eV, EI): *m/z* (%): 430 (8) [M^+], 416 (100) [M^+−BH_3], 73 (25) [$SiMe_3^+$]; elemental analysis calcd (%) for $C_{20}H_{28}BPS_2Si_2$ (430.5): C 55.80, H 6.56, S 14.90; found: C 55.92, H 6.57, S 14.89.

Synthesis of 13: $[Pd(cod)Cl_2]$ (0.12 g, 0.4 mmol) was added to a solution of **6** (0.34 g, 0.8 mmol) in $CHCl_3$ (30 mL) at room temperature and stirred for another 30 min. Subsequent evaporation of all volatiles under vacuum provided **13** as a yellow powder in quantitative yield (0.40 g, 99%). Recrystallization from toluene provided orange crystals suitable for X-ray structure analysis.

$^{31}P\{^1H\}$ NMR (162.0 MHz, $CDCl_3$): $\delta = 1.5$ ppm (8.9 (0.3 equiv)); ^1H NMR (400 MHz, $CDCl_3$): $\delta = 7.78$ (brm, 2H; *o*-Ph), 7.69 (br, 2H; *m*-Ph) (6.70 (0.3 equiv)), 7.33–7.22 (brm, 3H; Ar), 0.30 ppm (s, 18H; $Si(CH_3)_3$) (0.24 (0.3 equiv)); $^{13}C\{^1H\}$ NMR (100.6 MHz, $CDCl_3$): $\delta = 148.7$ (t, $^2J(C,P) = 7.5$ Hz; Ar), 143.3 (br; Ar), 139.9 (t, $J(C,P) = 26.5$ Hz; Ar), 135.8 (t, $^1J(C,P) = 5.6$ Hz; Ar), 132.9 (dd, $^1J(C,P) = 311.9$, 17.1 Hz; *ipso*-Ar), 132.7 (d, $J(C,P) = 7.2$ Hz; Ar), 130.6 (s; *p*-Ph), 128.6 (t, $^3J(C,P) = 5.6$ Hz; *m*-Ph), −0.2 ppm (s; SiC_3); elemental analysis calcd (%) for $C_{40}H_{50}Cl_2P_2PdS_4Si_4$ (1010.7): C 47.53, H 4.99, S 12.69; found: C 47.65, H 4.94, S 13.14.

Synthesis of 14: *n*BuLi (8 mL, 20 mmol) was added dropwise to a solution of 3,3′-5,5′-tetrabromobithiophene (**3**) (4.82 g, 10 mmol) in THF (100 mL) at −78 °C. The solution was stirred for 15 min at −78 °C and then tributyltin chloride (6.51 g, 20 mmol) was added dropwise to the reaction mixture at that temperature. The reaction mixture was allowed to warm slowly to room temperature and the solvent was subsequently removed under vacuum. The residue was taken up in pentane (ca. 60 mL) and filtered through neutral alumina. Evaporation of the volatiles under vacuum at elevated temperatures provided **14** as an orange oil (7.2 g, 88 % yield).

^{1}H NMR (500 MHz, $CDCl_3$): $\delta = 7.04$ (s/d, $^2J(H,Sn^{117/119}) = 21.4$ Hz, 2H; Ar-H), 1.58 (m, 12H; CH_2), 1.35 (m, 12H; CH_2), 1.13 (m, 12H; CH_2-Sn), 0.91 ppm (t, 18H; CH_3Bu); ^{13}C{^{1}H} NMR (125.6 MHz, $CDCl_3$): $\delta = 139.7$ (s; Ar-Ar), 138.1 (s/d, $^2J(C,Sn^{117/119}) = 21.1$ Hz; Ar-H), 134.6 (s; Ar-Sn), 112.8 (s; Ar-Br), 28.9 (s/d, $J(C,Sn^{117/119}) = 21.1$ Hz; CH_2), 27.2 (s/d, $J(C,Sn^{117/119}) = 59.5$ Hz; CH_2), 13.6 (s; CH_3), 11.0 ppm (s/d, $J(C,Sn^{117/119}) = 348.0$ Hz; CH_2Sn); MS (70 eV, EI): *m*/*z* (%): 902 (25) [M^+], 844 (60) [M^+−Bu], 313 (100) [$C_8H_{18}BrSn^+$], 57 (50) [Bu^+].

Synthesis of 15: *n*BuLi (1.6 mL, 4 mmol) was added dropwise to a solution of **14** (1.80 g, 2 mmol) and TMEDA (1.51 mL, 10 mmol) in Et_2O (50 mL) at −78 °C. Subsequently, $PhPCl_2$ (0.36 g, 2 mmol), dissolved in Et_2O (10 mL), was slowly added to the reaction mixture and the resulting suspension was allowed to warm quickly to room temperature. The solvent was then removed under vacuum, and the residue taken up in pentane (ca. 60 mL) and filtered through neutral alumina to remove LiCl and some brown impurities. The filtrate was evaporated to dryness at elevated temperatures and **15** was obtained as orange-brown oil (1.05 g, 62 % yield).

^{31}P{^{1}H} NMR (80.9 MHz, $CDCl_3$): $\delta = -28.0$ ppm; ^{1}H NMR (500 MHz, $CDCl_3$): $\delta = 7.39$ (br, 2H; *o*-Ph), 7.28 (br, 3H; *m*,*p*-Ph), 7.17 (s/d, $^2J(C,Sn^{117/119}) = 20.7$ Hz, 2H; Ar-H), 1.55 (m, 12H; CH_2), 1.34 (m, 12H; CH_2), 1.13 (m, 12H; CH_2Sn), 0.90 ppm (t, 18H; CH_3); ^{13}C{^{1}H} NMR (125.6 MHz, $CDCl_3$): $\delta = 148.0$ (d, $^1J(C,P) = 10.5$ Hz; *ipso*-Ar), 147.5 (d, $^2J(C,P) = 2.5$ Hz; Ar-Ar), 138.7 (d, $^3J(C,P) = 2.8$ Hz; Ar-Sn), 134.6 (d, s/d, $^3J(C,P) = 18.2$, $^2J(C,Sn^{117/119}) = 18.4$ Hz; Ar-H), 134.9 (d, $^1J(C,P) = 16.3$ Hz; *ipso*-Ph), 132.5 (d, $^1J(C,P) = 18.2$ Hz; *o*-Ph), 128.7 (s; *p*-Ph), 128.6 (d, $^4J(C,P) = 6.7$ Hz; *m*-Ph), 29.0 (s; CH_2), 27.3 (s; CH_2), 13.7 (s; CH_3), 11.0 ppm (s; CH_2Sn); ^{119}Sn{^{1}H} NMR (186.3 MHz, $CDCl_3$): $\delta = -36.7$ ppm; elemental analysis calcd (%) for $C_{38}H_{61}PS_2Sn_2$ (850.4): C 53.67, H 7.23, S 7.54; found: C 53.28, H 7.17, S 8.56.

Synthesis of 16: Hydrogen peroxide (0.5 g, 3.3 mmol, 30 % solution in H_2O) was added to a solution of **15** (2.55 g, 3 mmol) in THF (20 mL) at room temperature. The reaction mixture was stirred for 3 h. Subsequently, all volatile materials were removed under vacuum and the residue taken up in pentane and filtered through neutral alumina. Evaporation of the solvent under vacuum provided **16** as a yellow oil (2.36 g, 91 % yield). ^{31}P{^{1}H} NMR (80.9 MHz, $CDCl_3$): $\delta = 14.7$ ppm; ^{1}H NMR (500 MHz, $CDCl_3$): $\delta = 7.76$ (dd, $^3J(H,P) = 14.0$, $^3J(H,H) = 7.4$ Hz, 2H; *o*-Ph), 7.52 (td, $^3J(H,H) = 7.6$, $^4J(C,P) = 2.4$ Hz, 1H; *p*-Ph), 7.42 (td, $^3J(H,H) = 7.6$, $^3J(H,P) = 3.4$ Hz, 2H; *m*-Ph), 7.12 (d/dd, $^3J(H,P) = 2.1$, $^2J(C,Sn^{117/119}) = 19.6$ Hz, 2H; Ar-H), 1.54 (m, 12H; CH_2), 1.31 (m, 12H; CH_2), 1.10 (m, 12H; CH_2Sn), 0.89 ppm (t, 18H; CH_3); ^{13}C{^{1}H} NMR (125.6 MHz, $CDCl_3$): $\delta = 151.5$ (d, $^1J(C,P) = 30.0$ Hz; *ipso*-Ar), 141.8 (d, $^2J(C,P) = 12.5$ Hz; Ar-Ar), 140.6 (s; Ar-Sn), 133.4 (d, $^2J(C,P) = 12.5$ Hz; *o*-Ar), 132.0 (d, $^1J(C,P) = 2.9$ Hz; *p*-Ph), 132.0 (d, $^1J(C,P) = 69.9$ Hz; *ipso*-Ph), 131.0 (d, $^2J(C,P) = 11.5$ Hz; *o*-Ar), 128.7 (d, $^4J(C,P) = 13.4$ Hz; *m*-Ph), 28.9 (s; CH_2), 27.2 (s; CH_2), 13.6 (s; CH_3), 11.0 ppm (s, CH_2Sn); elemental analysis calcd (%) for $C_{38}H_{61}OPS_2Sn_2$ (866.4): C 52.68, H 7.10, S 7.40; found: C 51.86, H 7.02, S 6.96.

Synthesis of 18: Catalytic amounts of $[Pd(PPh_3)_4]$ and CuI were added to a solution of dithienophosphole **16** (1.73 g, 1.5 mmol) and 1,4-diiodo-2,5-bis(octyloxy)benzene **17** (0.88 g, 1.5 mmol) in NMP (80 mL). The light-yellow reaction mixture was then stirred for 48 h at 200 °C after which time the color changed to orange-red. The solution was then cooled to room temperature, the solvent evaporated under vacuum, and the resulting amorphous solid taken up in a small amount of THF (ca. 5 mL). The suspension was then filtered through a filter paper, precipitated into hexane and the residue dried under vacuum to yield **18** as a reddish brown powder (1.1 g).

^{31}P{^{1}H} NMR (202.3 MHz, $C_2D_2Cl_4$): $\delta \approx 14$ ppm; ^{1}H NMR (500 MHz, $C_2D_2Cl_4$): $\delta = 7.64$–6.90 (br; Ar-H), 3.95 (br; OCH_2), 1.71–0.88 ppm (br m; alkyl-H); ^{13}C{^{1}H} NMR (125.6 MHz, $C_2D_2Cl_4$): $\delta = 155.6$, 144.0, 142.1, 130.5, 128.4 (br; C_{Ar}), 69.6 (br; OCH_2), 31.6, 29.1, 26.6, 26.1, 22.5, 14.1, 13.5 ppm (C_{alkyl}).

Acknowledgements

The authors would like to thank Prof. Dr. J. Okuda for his generous support of this work. Financial support from the *Fonds der Chemischen Industrie, BMBF*, and from OTKA (Grant No. T 034675 and D 042216) is gratefully acknowledged. We thank Prof. Dr. U. Englert for the X-ray data collection and helpful discussions, Prof. Dr. U. Kölle for his assistance with the cyclovoltammetry, and A. Bartole-Scott (University of Toronto) for the GPC analyses. T.K. and L.N. acknowledge the generous allocation of computer time from NIIF/Hungary.

[1] a) F. Mathey, *Angew. Chem.* **2003**, *115*, 1616; *Angew. Chem. Int. Ed.* **2003**, *42*, 1578; b) Z. Jin, B. L. Lucht, *J. Organomet. Chem.* **2002**, *653*, 167; c) C.-W. Tsang, M. Yam, D. P. Gates, *J. Am. Chem. Soc.* **2003**, *125*, 1480; d) C.-W. Tsang, B. Baharloo, D. Riendl, M. Yam, D. P. Gates, *Angew. Chem.* **2004**, *116*, 5800; *Angew. Chem. Int. Ed.* **2004**, *43*, 5682; e) R. C. Smith, J. D. Protasiewicz, *J. Am. Chem. Soc.* **2004**, *126*, 2268; f) C. Hay, M. Hissler, C. Fischmeister, J. Rault-Berthelot, L. Toupet, L. Nyulászi, R. Réau, *Chem. Eur. J.* **2001**, *7*, 4222.

[2] See, for example: a) *Handbook of Oligo- and Polythiophenes* (Ed.: D. Fichou), Wiley-VCH, Weinheim, **1998**; b) *Conjugated Conducting Polymers*, *Vol. 102* (Ed.: H. Kiess), Springer, New York, **1992**.

[3] G. Tourillion, "Polythiophene and its Derivatives" in *Handbook of Conducting Polymers* (Ed.: T. A. Skotheim), Marcel Dekker, New York, **1986**.

[4] a) C. Hay, C. Fischmeister, M. Hissler, L. Toupet, R. Réau, *Angew. Chem.* **2000**, *112*, 1882; *Angew. Chem. Int. Ed.* **2000**, *39*, 1812; b) C. Hay, D. Le Vilain, V. Deborde, L. Toupet, R. Réau, *Chem. Commun.* **1999**, 345; c) C. Fave, T.-Y. Cho, M. Hissler, C.-W. Chen, T.-Y. Luh, C.-C. Wu, R. Réau, *J. Am. Chem. Soc.* **2003**, *125*, 9254; d) C. Fave, M. Hissler, T. Kárpáti, J. Rault-Berthelot, V. Deborde, L. Toupet, L. Nyulászi, R. Réau, *J. Am. Chem. Soc.* **2004**, *126*, 6058.

[5] a) D. Delaere, M. T. Nguyen, L. G. Vanquickenborne, *Phys. Chem. Chem. Phys.* **2002**, *4*, 1522; b) D. Delaere, M. T. Nguyen, L. G. Vanquickenborne, *J. Phys. Chem. A* **2003**, *107*, 838; c) J. Ma, S. Li, Y. Jiang, *Macromolecules* **2002**, *35*, 1109.

[6] a) E. Deschamps, L. Ricard, F. Mathey, *Angew. Chem.* **1994**, *106*, 1214; *Angew. Chem. Int. Ed. Engl.* **1994**, *33*, 1158; b) M.-O. Bévierre, F. Mercier, L. Ricard, F. Mathey, *Angew. Chem.* **1990**, *102*, 672; *Angew. Chem. Int. Ed. Engl.* **1990**, *29*, 655.

[7] a) S. S. H. Mao, T. D. Tilley, *Macromolecules* **1997**, *30*, 5566; b) Y. Morisaki, Y. Aiki, Y. Chujo, *Macromolecules* **2003**, *36*, 2594.

[8] J. Roncali, *Chem. Rev.* **1997**, *97*, 173.

[9] a) J. Ohshita, M. Nodono, H. Kai, T. Watanabe, A. Kunai, K. Komaguchi, M. Shiotani, A. Adachi, K. Okita, Y. Harima, K. Yamashita, M. Ishikawa, *Organometallics* **1999**, *18*, 1453; b) J. Ohshita, T. Sumida, A. Kunai, A. Adachi, K. Sakamaki, K. Okita, *Macromolecules* **2000**, *33*, 8890; c) J. Ohshita, H. Kai, T. Sumida, A. Kunai, A. Adachi, K. Sakamaki, K. Okita, *J. Organomet. Chem.* **2002**, *642*, 137.

[10] S. Kim, K.-H. Song, S. O. Kang, J. Ko, *Chem. Commun.* **2004**, 68.

[11] T. Benincori, V. Consonni, P. Grammatica, T. Pilati,, S. Rizzo, F. Pannicolo, R. Todeschini, G. Zotti, *Chem. Mater.* **2001**, *13*, 1665.

[12] a) D. D. Kenning, K. Ogawa, S. D. Rothstein, S. C. Rasmussen, *Polym. Mater. Sci. Eng.* **2002**, *86*, 59; b) K. Ogawa, S. C. Rasmussen, *J. Org. Chem.* **2003**, *68*, 2921.

[13] J. Ohshita, M. Nodono, T. Watanabe, Y. Ueno, A. Kunai, Y. Harima, K. Yamashita, M. Ishikawa, *J. Organomet. Chem.* **1998**, *553*, 487.

[14] G. Barbarella, L. Favaretto, G. Sotgiu, L. Antolini, G. Gigli, R. Cingolati, A. Bongini, *Chem. Mater.* **2001**, *13*, 4112.
[15] J.-P. Lampin, F. Mathey, *J. Organomet. Chem.* **1974**, *71*, 239.
[16] a) T. Baumgartner, T. Neumann, B. Wirges, *Angew. Chem.* **2004**, *116*, 6323; *Angew. Chem. Int. Ed.* **2004**, *43*, 6197; b) T. Baumgartner, *Macromol. Symp.* **2003**, *196*, 279.
[17] a) M. Pomerantz in *Handbook of Conducting Polymers*, 2nd ed., (Eds.: T. A. Skotheim, R. L. Elsenbaumer, J. R. Reynolds), Marcel Dekker, New York, **1998**, pp. 277–309; b) X. Zhang, A. J. Matzger, *J. Org. Chem.* **2003**, *68*, 9813; c) S. Y. Hong, J. M. Song, *J. Chem. Phys.* **1997**, *107*, 10607.
[18] a) A. N. Hughes, D. Kleemola, *J. Heterocycl. Chem.* **1976**, *13*, 1; b) W. Egan, R. Tang, G. Zon, K. Mislow, *J. Am. Chem. Soc.* **1971**, *93*, 6205.
[19] F. Mathey, *Chem. Rev.* **1988**, *88*, 429.
[20] A. Reed, P. von R. Schleyer, *J. Am. Chem. Soc.* **1990**, *112*, 1434.
[21] T. K. Miyamoto, Y. Matsuura, K. Okude, H. Ichida, *J. Organomet. Chem.* **1989**, *373*, C8.
[22] Obtained in a similar manner as **10a** by using **8** as the starting material.
[23] The observed disorder can be attributed to molecular motions—even at 110 K—within the crystal which lead to the displaced thiophene and silyl units.
[24] H. Nöth, B. Wrackmeyer, *Nuclear Magnetic Resonance Spectroscopy of Boron Compounds*, Springer, New York, **1978**.
[25] a) J. J. MacDougall, J. H. Nelson, F. Mathey, J. J. Mayerle, *Inorg. Chem.* **1980**, *19*, 709; b) J. Hydrio, M. Gouygou, F. Dallemer, G. G. A. Balavoine, J.-C. Daran, *J. Organomet. Chem.* **2002**, *643-644*, 19.
[26] M. Ogasawara, K. Yoshida, T. Hayashi, *Organometallics* **2001**, *20*, 1014.
[27] W. L. Wilson, J. Fischer, R. E. Wasylishen, K. Eichele, V. J. Catalano, J. H. Frederik, J. H. Nelson, *Inorg. Chem.* **1996**, *35*, 1486.
[28] P. B. Koster, F. van Bolhuis, G. J. Visser, *Acta Crystallogr.* **1970**, *26*, 1932.
[29] B. Valeur, *Molecular Fluorescence, Principles and Applications*, Wiley-VCH, Weinheim, **2002**.
[30] G. Barbarella, *Chem. Eur. J.* **2002**, *8*, 5073.
[31] D. T. McQuade, A. E. Pullen, T. M. Swager, *Chem. Rev.* **2000**, *100*, 2537.
[32] C. W. Bird, *Tetrahedron* **1985**, *41*, 1409.
[33] Z. Bao, W. K. Chan, L. Yu, *J. Am. Chem. Soc.* **1995**, *117*, 12426.
[34] Gaussian 98 (Revision A.5), M. J. Frisch, G. W. Trucks, H. B. Schlegel, G. E. Scuseria, M. A. Robb, J. R. Cheeseman, V. G. Zakrzewski, J. A. Montgomery, Jr., R. E. Stratmann, J. C. Burant, S. Dapprich, J. M. Millam, A. D. Daniels, K. N. Kudin, M. C. Strain, O. Farkas, J. Tomasi, V. Barone, M. Cossi, R. Cammi, B. Mennucci, C. Pomelli, C. Adamo, S. Clifford, J. Ochterski, G. A. Petersson, P. Y. Ayala, Q. Cui, K. Morokuma, D. K. Malick, A. D. Rabuck, K. Raghavachari, J. B. Foresman, J. Cioslowski, J. V. Ortiz, B. B. Stefanov, G. Liu, A. Liashenko, P. Piskorz, I. Komaromi, R. Gomperts, R. L. Martin, D. J. Fox, T. Keith, M. A. Al-Laham, C. Y. Peng, A. Nanayakkara, C. Gonzalez, M. Challacombe, P. M. W. Gill, B. G. Johnson, W. Chen, M. W. Wong, J. L. Andres, M. Head-Gordon, E. S. Replogle, J. A. Pople, Gaussian, Inc., Pittsburgh, PA, **1998**.
[35] W. Gordy, *J. Chem. Phys.* **1947**, *15*, 305.
[36] H. Meng, W. Huang, *J. Org. Chem.* **2000**, *65*, 3894.
[37] M. Fild, O. Stelzer, R. Schmutzler, *Inorg. Synth.* **1973**, *14*, 4.
[38] E. P. Kyba, *J. Am. Chem. Soc.* **1976**, *98*, 4805.
[39] D. Drew, J. R. Doyle, *Inorg. Synth.* **1972**, *13*, 52.
[40] C. Weder, M. S. Wrighton, *Macromolecules* **1996**, *29*, 5157.

Received: February 11, 2005
Published online: May 25, 2005

